Hindawi Publishing Corporation
The Scientific World Journal
Volume 2014, Article ID 342020, 8 pages
http://dx.doi.org/10.1155/2014/342020

*Research Article*

# Photocatalytic Degradation of DIPA Using Bimetallic Cu-Ni/$TiO_2$ Photocatalyst under Visible Light Irradiation

**Nadia Riaz,[1,2] Mohamad Azmi Bustam,[1] Fai Kait Chong,[3] Zakaria B. Man,[1] Muhammad Saqib Khan,[2,3] and Azmi M. Shariff[1]**

[1] *Chemical Engineering Department, Universiti Teknologi PETRONAS, 31750 Tronoh, Malaysia*
[2] *COMSATS Institute of Information Technology, Tobe Camp, University Road, Abbottabad 22060, Pakistan*
[3] *Fundamental & Applied Sciences Department, Universiti Teknologi PETRONAS, 31750 Tronoh, Malaysia*

Correspondence should be addressed to Nadia Riaz; nadiariazz@gmail.com
and Mohamad Azmi Bustam; azmibustam@petronas.com.my

Received 26 March 2014; Accepted 9 June 2014; Published 29 June 2014

Academic Editor: Degang Fu



Bimetallic Cu-Ni/$TiO_2$ photocatalysts were synthesized using wet impregnation (WI) method with $TiO_2$ (Degussa-P25) as support and calcined at different temperatures (180, 200, and 300°C) for the photodegradation of DIPA under visible light. The photocatalysts were characterized using TGA, FESEM, UV-Vis diffuse reflectance spectroscopy, fourier transform infrared spectroscopy (FTIR) and temperature programmed reduction (TPR). The results from the photodegradation experiments revealed that the Cu-Ni/$TiO_2$ photocatalysts exhibited much higher photocatalytic activities compared to bare $TiO_2$. It was found that photocatalyst calcined at 200°C had the highest photocatalyst activities with highest chemical oxygen demand (COD) removal (86.82%). According to the structural and surface analysis, the enhanced photocatalytic activity could be attributed to its strong absorption into the visible region and high metal dispersion.

## 1. Introduction

Semiconductor photocatalysis has been investigated extensively for light-stimulated degradation of pollutants, particularly for complete destruction of toxic and nonbiodegradable compounds into carbon dioxide and inorganic constituents [1]. The fundamentals of semiconductor photocatalysis and its application to the removal of chemical pollutants have been extensively reviewed [2]. Several semiconductors exhibit bandgap energies suitable for photocatalytic degradation of contaminants. Among the photocatalysts applied, titanium dioxide is one of the most widely employed photocatalytic semiconducting materials because of the peculiarities of chemical inertness, nonphotocorrosion, low cost, and nontoxicity. Doping semiconductors with various metal ions, composite semiconductors, deposition of transition metals, and oxygen reduction catalysts can be employed to enhance photocatalytic efficiency [3]. The photocatalytic process is characterized by the production of $^{\bullet}OH$ radicals which are able to oxidize and mineralize organic compounds [4].

However, a serious limitation for the application of $TiO_2$ semiconductor in heterogeneous photocatalysis is the requirement of UV light to promote the electron transference process due to its wide bandgap (about 3.2 eV). For the fabrication of visible light active photocatalysts, the modification of semiconductors by the addition of transition metals and nonmetal doping are the commonly adopted ways [5–7]. Modification of titania by doping using transition metals has often been used to enhance its photocatalytic activity and to extend its absorption wavelength from the UV to visible region [8]. The use of Cu and Ni as bimetallic catalysts supported on different semiconductor materials has been reported as the effective method to improve the efficiency of various reactions like carbon dioxide hydrogenation [9], steam reforming of methane [10], liquid-phase glycerol hydrogenolysis by formic acid over Ni-Cu/$Al_2O_3$ catalysts

[11], decomposition of methane over Ni-$SiO_2$ and Ni-Cu-$SiO_2$ catalysts [12], photocatalytic reduction of nitrate [13], azo dye degradation using Cu-Zn/$TiO_2$ [8], Ni/$TiO_2$ [14] and Cu-Fe/$TiO_2$ [15] for methyl orange degradation, and Cu/$TiO_2$ for Orange II degradation [16].

The objective of the present work is to investigate the photocatalytic degradation of diisopropanolamine (DIPA) in the presence of Cu-Ni/$TiO_2$ photocatalyst under visible light source. The introduction of Cu and Ni was with the intention to reduce the bandgap of the photocatalyst for enhanced visible light absorption. In order to obtain a better understanding, we investigated the influence of various parameters that may affect the photodegradation of DIPA.

## 2. Experimental

*2.1. Materials.* Copper nitrate trihydrate, $Cu(NO_3)_2{\cdot}3H_2O$, and nickel nitrate hexahydrate, $Ni(NO_3)_2{\cdot}6H_2O$ (Acros brand > 98% purity), were used as dopant metal salts. Titanium dioxide, $TiO_2$ (Degussa-P25 80% anatase, 20% rutile), was used as the support which also acts as the semiconductor in photocatalysis. Diisopropanolamine (DIPA) (Merck, Germany) was used as the model alkanolamine for photocatalytic degradation study. All chemicals were used as received.

*2.2. Photocatalyst Preparation.* Bimetallic Cu-Ni/$TiO_2$ photocatalysts with 10 wt% total metal loading and 9Cu : 1Ni mass composition were prepared using wet impregnation (WI) method with $TiO_2$ as support. 9Cu : 1Ni mass composition and 10 wt% metal loading were selected based on the results reported in [18]. To prepare photocatalysts using WI method, support was added into the metal salt solution. The suspension was stirred for 1 hour before the solvent was evaporated in a water bath at 80°C until a thick paste was obtained. This paste was then dried in an oven at 120°C for 18 hours. The dried photocatalyst was ground with a mortar and pestle, kept in air-tight glass bottle (to avoid moisture) as raw photocatalyst, and stored in a desiccator at room temperature prior to calcination.

*2.3. Characterization.* The photocatalysts were characterized using different characterization techniques to understand the chemical and physical properties and then to relate these properties to their photocatalytic performance. In order to estimate suitable calcinations temperatures for the raw photocatalysts, thermal gravimetric analysis (TGA) was carried out using Perkin Elmer (Pyris 1 TGA) instrument. The morphology of the photocatalysts such as crystallite particle shape and size distribution was analyzed using FESEM (Supra55VP). Reflectance spectrums were recorded at 190–800 nm wavelength using DR-UV-Vis spectrophotometer (Shimadzu Lambda 900). Barium sulphate ($BaSO_4$) powder was used as a standard, an internal reference. Fourier transform infrared spectroscopy (FTIR, Shimadzu FTIR-8400S) analyses were carried out to identify species present in the photocatalysts. A small amount of photocatalyst was grained together with 50 mg of IR-grade KBr and pressed into pellet using a hydraulic hand press. Later the pellet was placed in the sample holder and scanned at 4000 $cm^{-1}$ to 400 $cm^{-1}$. KBr was used as the background file. The temperature programmed reduction (TPR) analyses were conducted in order to determine reducibility of the photocatalysts and metal dispersion in photocatalysts using Thermo Finnigan equipment (TPDRO 1100). Prior to reduction, the sample was pretreated under nitrogen at 110°C with a flow rate of 20 mL $min^{-1}$ and ramp rate of 10°C $min^{-1}$ and finally holding at 110°C for 30 minutes to eliminate moisture before cooling to room temperature. TPR analysis was carried out in 5% $H_2$ in $N_2$ with a flow rate of 20 mL $min^{-1}$. Samples were heated with a ramp rate of 20°C $min^{-1}$ from 40°C to 500°C and holding at 500°C for 10 minutes. The reduction profile was shown in a plot of hydrogen consumption as a function of linearity temperature.

*2.4. Measurements of Photocatalytic Activities.* Photocatalytic activity of the prepared photocatalysts was evaluated by monitoring the photocatalytic degradation of alkanolamine in aqueous solution under visible light irradiation. For a typical experiment, photocatalysts were weighed and mixed with distilled water and then ultrasonicated for 5 min using sonicator followed by the addition of DIPA solution (final concentration of 100 ppm, photocatalyst loading of 1 g·$L^{-1}$, and total volume of 100 mL). The suspension was stirred in the dark for 30 minutes and later this suspension was illuminated for 1 h using the 500 W halogen lamp as the visible light source. Reaction study was carried out at atmospheric pressure and room temperature (at 25 ± 1°C) that was controlled by continuous cooling air. The apparatus used for reaction study has been described elsewhere [14]. Samples were collected at different intervals of time (min) and were immediately centrifuged twice to remove suspended solid photocatalyst and monitored for further analysis. For the photodegradation experiments at different pH values, the initial pH of the reaction suspension was adjusted by the addition of NaOH or HCl solutions.

The degradation of alkanolamine was measured by chemical oxygen demand (COD) using Hach UV-Vis spectrophotometer (DR 39000) to measure the COD/TOC concentration (mg·$L^{-1}$) for the reaction samples. In order to determine the mineralization efficiency of photocatalyst, COD removal (%) was calculated as follows:

$$\text{COD removal } (\%) = \left(\frac{\text{COD}_0 - \text{COD}_t}{\text{COD}_0}\right) \times 100, \quad (1)$$

where $COD_0$ is the initial COD in ppm and $COD_t$ is the final COD concentration in ppm at different time intervals during reaction.

## 3. Results and Discussion

*3.1. Photocatalyst Preparation and Characterization.* Bimetallic Cu-Ni/$TiO_2$ photocatalysts were prepared using wet impregnation (WI) method with $TiO_2$ as support. Total metal loading (10 wt%) and Cu : Ni mass composition (9Cu-1Ni) were fixed based on the optimization results reported by our research group [18]. Prepared photocatalysts were

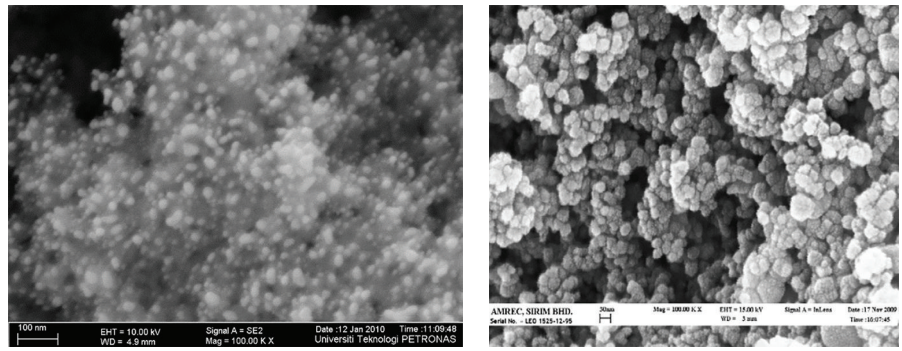


(a) (b)

Figure 1: FESEM micrograph of (a) bare $TiO_2$ and (b) Cu-Ni/$TiO_2$ photocatalysts (at magnification 100KX) [17].

characterized using different characterization techniques in order to relate the physicochemical properties with the photocatalyst performance.

Results from TGA were reported as thermograms as shown in our previous work [17], which are plots of the relative weight of the photocatalyst versus temperature. Based on the TGA results, calcination was conducted at selected temperatures for 1 h duration. The calcined photocatalysts were given denotation: $x$Cu-$y$Ni-$T$ where "$x$" and "$y$" represent the mass composition of Cu and Ni, respectively, with "$x$" + "$y$" = 10, while "$T$" represents calcination temperature in °C. Photocatalysts were calcined at three different calcination temperatures: 180, 200, and 300°C.

FESEM (field-emission scanning electron microscopy) micrographs for the bare $TiO_2$ and photocatalysts calcined at 200°C are presented in Figure 1. The micrographs of the Cu-Ni/$TiO_2$ photocatalysts clearly depict uniform distribution with spherical morphologies and slight agglomeration ranging from 11 to 40 nm. Comparing micrographs of bare $TiO_2$ with bimetallic it is clear that addition of Cu-Ni to bare $TiO_2$ can help to enhance the particle shape and size. The photocatalysts samples were partly composed of clusters containing composite nanoparticles adhering to each other. The agglomeration might be due to sintering during calcination process. From the EDX spectrum it was observed that metal oxides were well dispersed over the $TiO_2$ support.

Modification with metal has shifted the absorption spectrum of $TiO_2$ into visible region. The diffuse reflectance UV-visible (DR-UV-Vis) spectra of bare $TiO_2$ (Figure 2) showed absorption peaks ranging from 190 nm to 400 nm, similar to that observed in our previous studies [18–20]. The shift in the absorption spectrum has been observed for the synthesized photocatalysts. Impregnation method has also reported previously that this method can also shift the absorption spectrum of $TiO_2$ [21]. The shift might not possibly be caused by the change in the bandgap but rather might be by the impurity of energy level as the metal is spread on the surface of $TiO_2$ photocatalyst.

Results of physical characterization by diffuse reflectance UV-visible (DR-UV-Vis) spectra and FESEM indicate that the copper and nickel metal were highly dispersed and interacted with the $TiO_2$ support. High dispersion and low bandgap

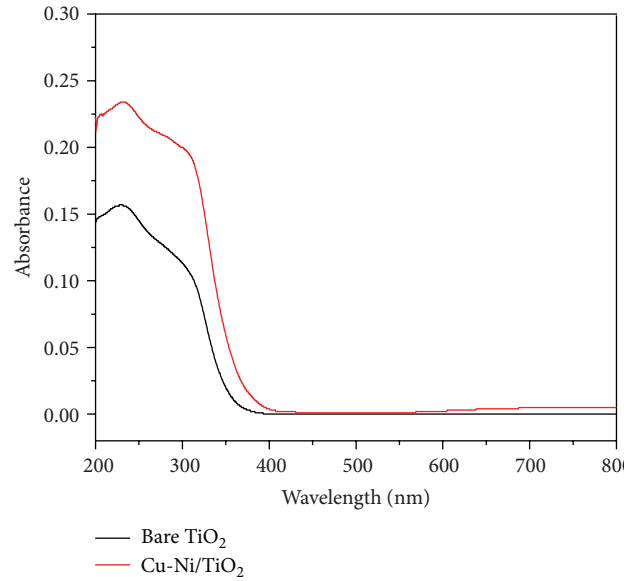


Figure 2: Absorption spectra for bare $TiO_2$ and bimetallic Cu-Ni/$TiO_2$ photocatalysts.

energy together play synergetic effect for photodegradation performance of the photocatalysts under visible light irradiation. The lower bandgap energy of bimetallic photocatalysts compared to that of bare $TiO_2$ and monometallics also becomes a reason of its higher activity.

FTIR spectra of bare $TiO_2$ and raw and calcined photocatalysts (10 wt% Cu-1Ni/$TiO_2$-200) are shown in Figure 3. Several absorption peaks were observed. The broad band around 3400 $cm^{-1}$ was attributed to O–H stretching and the peak near 1600 $cm^{-1}$ was attributed to H–O–H bending and related to physically absorbed moisture [19, 22]. The IR band observed from 400 to 900 $cm^{-1}$ corresponds to the Ti–O stretching vibrations [23–25]. The intense peak at 1384 $cm^{-1}$ was ascribed to nitrate ($NO_3^-$) group which is present in all the spectra. The presence of nitrate band was also observed by Mohan [26] and Li and Inui [27]. They mentioned that the nitrate will always be present when nitrate salts are used

Table 1: Assignment of absorption peaks observed in FTIR spectra of bare $TiO_2$ and Cu-Ni/$TiO_2$ photocatalysts.

| Peaks ($cm^{-1}$) | Possible assignment | Related process occurring |
|---|---|---|
| 1600 | H–O–H bending | Physically adsorbed moisture |
| 3400 | O–H stretching of hydroxyl group | |
| 1384 | $NO_3^-$ anion | Presence of nitrate |

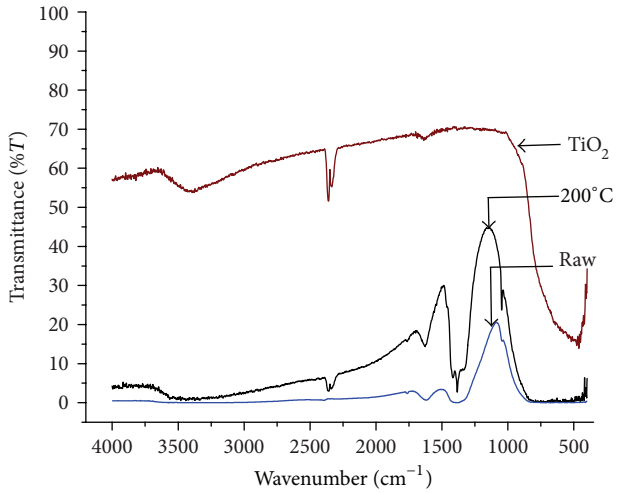


Figure 3: FTIR spectra of bare $TiO_2$ and Cu-Ni/$TiO_2$ photocatalysts (raw and calcined at 200°C).

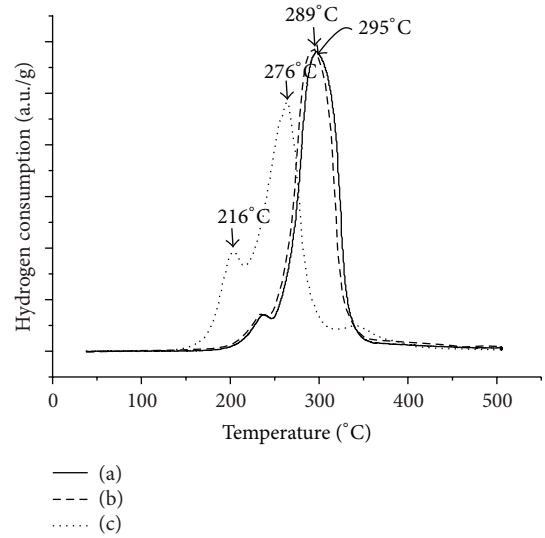


Figure 4: The TPR profiles of Cu-Ni/$TiO_2$ photocatalysts calcined at different temperatures: (a) 200, (b) 180, and (c) 300°C.

Table 2: Summary of the hydrogen consumption and the reduction temperature of the photocatalysts.

| Photocatalyst | Reduction peak (°C) | Amount of hydrogen consumed ($\mu$mol·$g^{-1}$) |
|---|---|---|
| 180°C | 295 | 1877.0 |
| | 361 | 1939.9 |
| 200°C | 289 | 1879.3 |
| | 357 | 1938.2 |
| 300°C | 216 | 345.79 |
| | 276 | 1436.2 |
| | 355 | 158.98 |

as precursors. Possible assignment of the peaks observed in FTIR spectra of bare $TiO_2$ and Cu : Ni/$TiO_2$ photocatalysts is shown in Table 1.

Temperature programmed reduction (TPR) was used in order to characterize the Cu-Ni/$TiO_2$ photocatalyst with respect to the type of metal oxide species present, either copper oxide, nickel oxide, or copper-nickel mixed oxide, and the degree of interaction of the oxides with $TiO_2$ support [19]. The summary of the amount of hydrogen consumed and reduction temperature of different photocatalysts is shown in Table 2. The TPR profiles of the bimetallic Cu-Ni/$TiO_2$ photocatalysts with different calcination temperatures are presented in Figure 4. The higher reduction peaks at 295°C were ascribed to bulk CuO phases that include large clusters and bulk CuO. The reduction profile of bimetallic Cu-Ni/$TiO_2$-200 showed a shoulder around 220–240°C and one main reduction peak at 289°C, which might be attributed to the reduction of Cu-Ni mixed oxide instead of individual oxide. Higher reduction temperatures are attributed to the reduction of NiO with strong interaction with $TiO_2$ [28]. The distinct peak observed at 289°C for 9Cu : 1Ni-180 might be attributed to the reduction of Cu-Ni mixed oxide instead of individual oxide [29]. It was also found that the presence of Cu lowered the reduction temperature of Ni. Li et al. [30] observed the same behavior as the bimetallic Cu-Ni/$TiO_2$. The addition of Cu enhanced the reduction of Ni; thereby, it can be concluded that the reducibility of bimetallic Cu-Ni is controlled by the amount of Cu. However, the presence of Cu-, Ni-, and mixed Cu-Ni species was not detected due to high dispersion of the metal particle on $TiO_2$. The TPR profile of photocatalyst is in good agreement with the results shown by FESEM that the Cu- species was highly dispersed on $TiO_2$ photocatalyst.

### 3.2. Photocatalytic Activity of Cu-Ni/$TiO_2$ Photocatalysts

*3.2.1. Effect of Irradiation Time.* Photocatalytic degradation of DIPA under visible light using bimetallic Cu-Ni/$TiO_2$ photocatalysts is displayed in Figure 5. COD removal using Cu-Ni/$TiO_2$ photocatalysts calcined at different calcination temperatures was calculated in terms of % COD removal. It is evident that the percentage of mineralization increases with

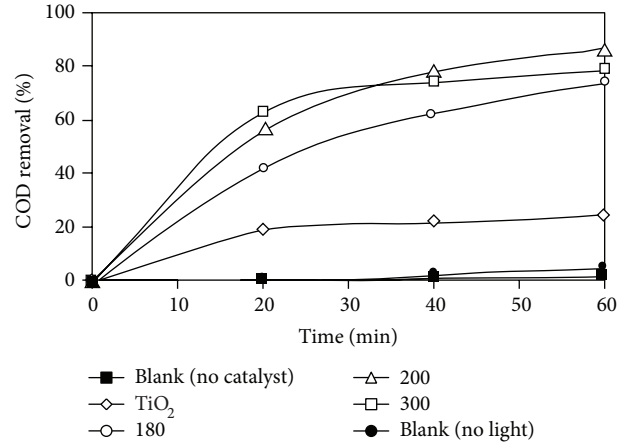


Figure 5: Photocatalytic degradation of DIPA under visible light using bimetallic Cu-Ni/$TiO_2$ photocatalysts (calcination temperatures = 180, 200, and 300°C; DIPA concentration = 100 ppm; reaction temperature = room temperature 23 ± 1; reaction volume = 100 mL; irradiation duration = 60 min; light source = 500 W halogen lamp; photocatalyst loading = 1 g·$L^{-1}$).

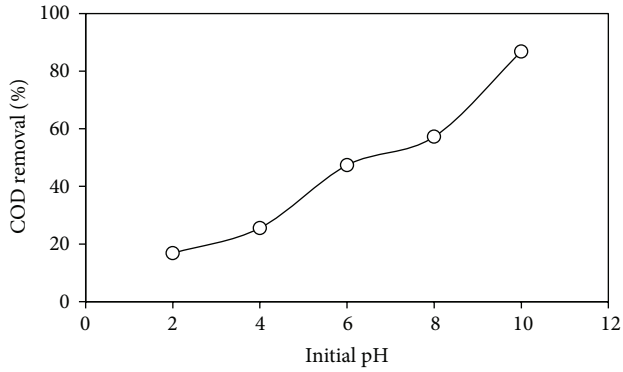


Figure 6: Effect of pH on photodegradation of DIPA using Cu-Ni/$TiO_2$ photocatalysts (photocatalysts loading = 1 g·$L^{-1}$; DIPA concentration = 100 ppm; irradiation time = 1 h).

irradiation time for photocatalysts calcined at different temperatures. The highest COD removal (%) was for photocatalyst calcined at 200°C. However, for photocatalyst calcined at 180 and 300°C and bare $TiO_2$, degradation was comparatively very slow with 74.16, 78.72, and 24.47% COD removal.

*3.2.2. Effect of pH.* The pH influences the characteristics of the photocatalyst surface charge, so pH of the solution is a significant parameter in performing the reaction on surface of $TiO_2$ particles for the photocatalytic degradation of organic pollutants [31]. The photodegradation of DIPA in the presence of 10 wt% Cu-Ni/$TiO_2$ photocatalysts is in the range between 2 and 12 as shown in Figure 6. From the previous studies, it is very clear that pH of a solution influences the surface charges of $TiO_2$ affecting the interfacial electron transfer and the photoredox process [32]. The point of zero charge (PZC) of $TiO_2$ is 6.25 and its surface is predominately

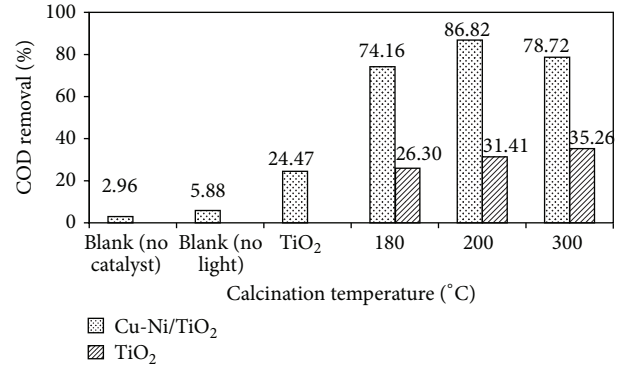


Figure 7: Effect of calcination temperature on photodegradation of DIPA using bare $TiO_2$ and Cu-Ni/$TiO_2$ photocatalysts (photocatalysts loading = 1 g·$L^{-1}$; DIPA concentration = 100 ppm; calcination temperature = 180, 200, and 300°C; irradiation time = 1 h).

positively charged below PZC and negatively charged above PZC. Alkanolamines are mostly protonated at pH 9 or below [31, 33]. From Figure 6, it is clear that the photodegradation increases with the increase in pH. This might be attributed to the increase in the number of $OH^-$ ions at the surface of $TiO_2$; hence, at acidic pH values, the particle surface is positively charged and active species like hydroxyl radical may not be adsorbed onto the positively charged $TiO_2$ surface, resulting in a decreased photodegradation. Results are in agreement with the previous studies [31, 33] which reported enhanced photodegradation at alkaline pH.

*3.2.3. Effect of Calcination Temperature.* Photocatalysts calcined at 180, 200, and 300°C were screened for photodegradation of 100 ppm DIPA under visible light irradiation. The % COD removal for different calcination temperatures was 74.16%, 86.82%, and 78.72% for photocatalysts calcined at 180, 200, and 300°C, respectively, as shown in Figure 7. The highest COD (%) removal was obtained for the photocatalysts calcined at 200°C. The results also indicate that the photocatalytic activity of synthesized titania decreased with the increased calcination temperature. Yu and coresearchers [34] also reported that a significant decrease in the photocatalytic activity of titania nanopowder calcined at higher temperature may be attributed to the growth of particle and result in the reduction of contact area of particles for photocatalytic reaction. The improvement of photocatalytic activity compared with commercial materials can be associated with the combined increase of crystallinity with the preservation of a relatively large surface area based on the existence of mesopores [35].

*3.2.4. Effect of Photocatalyst Loading.* Effect of photocatalyst amount on the photodegradation of DIPA is shown in Figure 8. Photocatalysts loading was in the range of 100–1000 g·$L^{-1}$. COD removal (%) was increased with increasing photocatalyst amount, indicating the availability of active sites on the photocatalyst surface for the adsorption of pollutant.

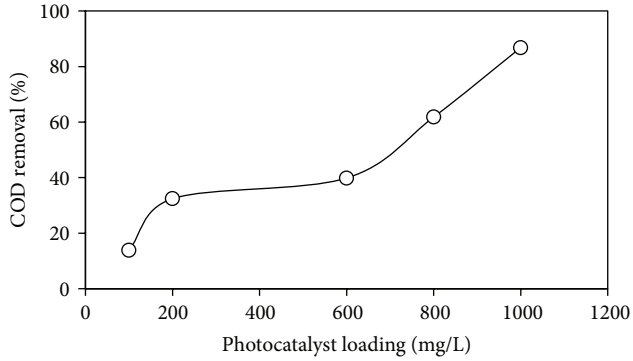


Figure 8: Effect of photocatalyst loading on photodegradation of DIPA using Cu-Ni/$TiO_2$ photocatalysts (photocatalysts loading = 100–1000 g·$L^{-1}$; calcination temperature = 200°C; DIPA concentration = 100 ppm; irradiation time = 1 h).

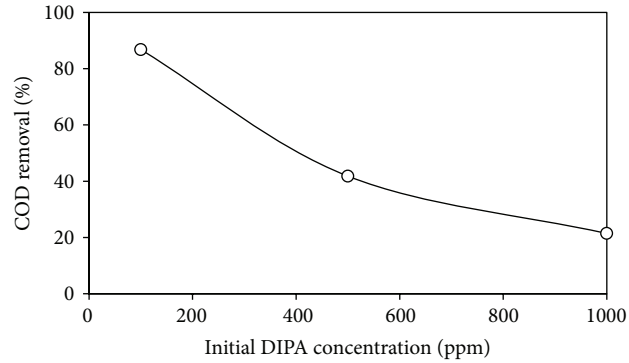


Figure 9: Effect of initial DIPA concentration on % COD removal using Cu-Ni/$TiO_2$ photocatalysts (photocatalysts loading = 1 g·$L^{-1}$; calcination temperature = 200°C; DIPA concentration = 100–1000 ppm; irradiation time = 1 h).

*3.2.5. Effect of Initial DIPA Concentration.* Effect of initial DIPA concentration that was studied by fixing the photocatalyst amount (based on the optimum photocatalyst loading 1 g·$L^{-1}$) on the photodegradation of DIPA is shown in Figure 9. COD removal (%) decreased with increasing initial DIPA concentration (100–100 ppm) indicating that as the pollutant concentration increases more organic substances are adsorbed on the surface of $TiO_2$, whereas less number of photons are available to reach the catalyst surface and therefore less $^{\bullet}OH$ radicals are formed, thus causing an inhibition in degradation percentage [36].

*3.2.6. Effect of Cu-Ni Codeposition.* The photocatalytic activities of the 10 wt% monometallic and bimetallic Cu, Ni, and Cu-Ni photocatalysts are presented in Figure 10. From the results, it is clear that the ratio of metal content in bimetallic catalysts plays a significant role in photocatalytic activity. The optimum COD removal (%) was obtained from bimetallic Cu-Ni/$TiO_2$ photocatalysts with 86.82%. For the monometallic photocatalysts, Cu/$TiO_2$ displayed better performance compared to Ni/$TiO_2$. However, their performance was lower than that of bimetallic Cu-Ni/$TiO_2$ and higher compared to that of bare $TiO_2$. In present study it was found that the addition of small amount of Ni enhanced the activity of bimetallic photocatalyst compared to those of monometallics; this might be due to synergetic effect of two different metals [37]. The presence of Cu and Ni plays a significant role in reduction of electron hole recombination by trapping electron and hole simultaneously. In particular Ni can enhance the hole trap thus retarded recombination reaction [18].

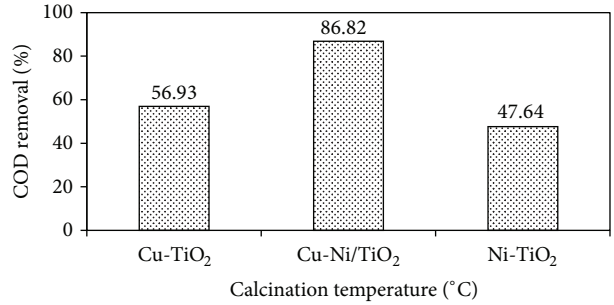


Figure 10: Effect of Cu-Ni codeposition on % COD removal using Cu/$TiO_2$, Ni/$TiO_2$, and Cu-Ni/$TiO_2$ photocatalysts (photocatalysts loading = 1 g·$L^{-1}$; calcination temperature = 200°C; DIPA concentration = 100 ppm; irradiation time = 1 h).

## 4. Conclusions

Surface modification of $TiO_2$ with copper and nickel had been successfully carried out using wet impregnation (WI) method with $TiO_2$ as support. Compared with the commercial reference, bare $TiO_2$ P25, the diffuse reflectance spectra suggest that the photoabsorption of Cu-Ni/$TiO_2$ photocatalysts is extended to the visible region. It is assumed that these Cu-Ni photocatalysts have induced impurity levels between the conduction and valence band of $TiO_2$, leading to narrower bandgap and enhancing the visible light absorption. The effect of process parameters such as irradiation duration (1 h), initial pH (pH range of 2–12), photocatalyst calcination temperature (180, 200, and 300°C), photocatalyst loading (0.1–1 g·$L^{-1}$), and initial DIPA concentration (100–100 ppm) has been investigated. The photocatalyst activity is directly related to photocatalysts loading suggesting that, for highly concentrated wastewater, dilution is a necessary step prior to the photodegradation step. Based on the results from the present study, the as-prepared highly active Cu-Ni/$TiO_2$ photocatalysts may have a great potential for photocatalytic water purification, particularly the elimination of toxic aromatic compounds under simulated solar light irradiation.

## Conflict of Interests

The authors declare that there is no conflict of interests regarding the publication of this paper.

## Acknowledgment

This work is part of a project entitled "Treatment of waste from $CO_2$ removal system by photocatalytic oxidation" funded by Universiti Teknologi PETRONAS, Malaysia.

## References

[1] M. R. Hoffmann, S. T. Martin, W. Choi, and D. W. Bahnemann, "Environmental applications of semiconductor photocatalysis," *Chemical Reviews*, vol. 95, no. 1, pp. 69–96, 1995.

[2] A. Mills and S. Le Hunte, "An overview of semiconductor photocatalysis," *Journal of Photochemistry and Photobiology A: Chemistry*, vol. 108, no. 1, pp. 1–35, 1997.

[3] O. Carp, C. L. Huisman, and A. Reller, "Photoinduced reactivity of titanium dioxide," *Progress in Solid State Chemistry*, vol. 32, no. 1-2, pp. 33–177, 2004.

[4] S. Malato, P. Fernández-Ibáñez, M. I. Maldonado, J. Blanco, and W. Gernjak, "Decontamination and disinfection of water by solar photocatalysis: recent overview and trends," *Catalysis Today*, vol. 147, no. 1, pp. 1–59, 2009.

[5] C. Yu, W. Zhou, K. Yang, and G. Rong, "Hydrothermal synthesis of hemisphere-like F-doped anatase $TiO_2$ with visible light photocatalytic activity," *Journal of Materials Science*, vol. 45, no. 21, pp. 5756–5761, 2010.

[6] C. Yu and J. C. Yu, "A simple way to prepare C-N-codoped $TiO_2$ photocatalyst with visible-light activity," *Catalysis Letters*, vol. 129, no. 3-4, pp. 462–470, 2009.

[7] C. Yu, J. C. Yu, and M. Chan, "Sonochemical fabrication of fluorinated mesoporous titanium dioxide microspheres," *Journal of Solid State Chemistry*, vol. 182, no. 5, pp. 1061–1069, 2009.

[8] D. Zhang and F. Zeng, "Photocatalytic oxidation of organic dyes with visible-light-driven codoped $TiO_2$ photocatalysts," *Russian Journal of Physical Chemistry A: Focus on Chemistry*, vol. 85, no. 6, pp. 1077–1083, 2011.

[9] Y. Liu and D. Liu, "Study of bimetallic Cu-Ni/$\gamma$-$Al_2O_3$ catalysts for carbon dioxide hydrogenation," *International Journal of Hydrogen Energy*, vol. 24, no. 4, pp. 351–354, 1999.

[10] T.-J. Huang and S.-Y. Jhao, "Ni-Cu/samaria-doped ceria catalysts for steam reforming of methane in the presence of carbon dioxide," *Applied Catalysis A: General*, vol. 302, no. 2, pp. 325–332, 2006.

[11] I. Gandarias, J. Requies, P. L. Arias, U. Armbruster, and A. Martin, "Liquid-phase glycerol hydrogenolysis by formic acid over Ni-Cu/$Al_2O_3$ catalysts," *Journal of Catalysis*, vol. 290, pp. 79–89, 2012.

[12] M. J. Lázaro, Y. Echegoyen, I. Suelves, J. M. Palacios, and R. Moliner, "Decomposition of methane over Ni-$SiO_2$ and Ni-Cu-$SiO_2$ catalysts: effect of catalyst preparation method," *Applied Catalysis A: General*, vol. 329, pp. 22–29, 2007.

[13] W. Gao, R. Jin, J. Chen et al., "Titania-supported bimetallic catalysts for photocatalytic reduction of nitrate," *Catalysis Today*, vol. 90, no. 3-4, pp. 331–336, 2004.

[14] D. Zhang, "Chemical synthesis of Ni/$TiO_2$ nanophotocatalyst for UV/visible light assisted degradation of organic dye in aqueous solution," *Journal of Sol-Gel Science and Technology*, vol. 58, no. 1, pp. 312–318, 2011.

[15] D. Zhang, "Enhanced photocatalytic activity for titanium dioxide by co-modification with copper and iron," *Transition Metal Chemistry*, vol. 35, no. 8, pp. 933–938, 2010.

[16] R. S. K. Wong, J. Feng, X. Hu, and P. L. Yue, "Discoloration and mineralization of non-biodegradable azo dye orange II by copper-doped $TiO_2$ nanocatalysts," *Journal of Environmental Science and Health A: Toxic/Hazardous Substances and Environmental Engineering*, vol. 39, no. 10, pp. 2583–2595, 2004.

[17] N. Riaz, C. Fai Kait, B. Kanti Dutta, M. Saqib Khan, and E. Nurlaela, "Effect of photocatalysts preparation methods and light source on Orange II photocatalytic degradation," in *Proceedings of the 2nd International Conference on Environmental Science and Technology*, pp. 111–117, Singapore, 2011.

[18] N. Riaz, F. K. Chong, B. K. Dutta, Z. B. Man, M. S. Khan, and E. Nurlaela, "Photodegradation of Orange II under visible light using Cu-Ni/$TiO_2$: effect of calcination temperature," *Chemical Engineering Journal*, vol. 185-186, pp. 108–119, 2012.

[19] L. S. Yoong, F. K. Chong, and B. K. Dutta, "Development of copper-doped $TiO_2$ photocatalyst for hydrogen production under visible light," *Energy*, vol. 34, no. 10, pp. 1652–1661, 2009.

[20] E. Nurlaela, F. K. Chong, B. K. Dutta, and N. Riaz, "Bimetallic Cu-Ni/$TiO_2$ as photocatalyst for hydrogen production from water," in *Proceedings of the International Conference on Fundamental and Applied Sciences (ICFAS '10)*, Convention Center, Kuala Lumpur, Malaysia, 2010.

[21] A. di Paola, G. Marcì, L. Palmisano et al., "Preparation of polycrystalline $Tio_2$ photocatalysts impregnated with various transition metal ions: characterization and photocatalytic activity for the degradation of 4-nitrophenol," *The Journal of Physical Chemistry B*, vol. 106, no. 3, pp. 637–645, 2002.

[22] D. Li, H. Haneda, S. Hishita, and N. Ohashi, "Visible-light-driven nitrogen-doped $TiO_2$ photocatalysts: effect of nitrogen precursors on their photocatalysis for decomposition of gas-phase organic pollutants," *Materials Science and Engineering B: Solid-State Materials for Advanced Technology*, vol. 117, no. 1, pp. 67–75, 2005.

[23] X. Yan, J. He, D. G. Evans, Y. Zhu, and X. Duan, "Preparation, characterization and photocatalytic activity of $TiO_2$ formed from a mesoporous precursor," *Journal of Porous Materials*, vol. 11, no. 3, pp. 131–139, 2004.

[24] R. Linacero, J. Aguado-Serrano, and M. L. Rojas-Cervantes, "Preparation of mesoporous $TiO_2$ by the sol-gel method assisted by surfactants," *Journal of Materials Science*, vol. 41, no. 8, pp. 2457–2464, 2006.

[25] K. Porkodi and S. D. Arokiamary, "Synthesis and spectroscopic characterization of nanostructured anatase titania: a photocatalyst," *Materials Characterization*, vol. 58, no. 6, pp. 495–503, 2007.

[26] J. Mohan, *Organic Spectroscopy Principles and Applications*, Alpha Science International, Harrow, UK, 2nd edition, 2007.

[27] J. L. Li and T. Inui, "Characterization of precursors of methanol synthesis catalysts, copper/zinc/aluminum oxides, precipitated at different pHs and temperatures," *Applied Catalysis A: General*, vol. 137, no. 1, pp. 105–117, 1996.

[28] M. D. Romero, J. A. Calles, A. Rodriguez, and J. C. Cabanelas, "The influence of calcination treatment over bifunctional Ni/HZSM-5 catalysts," *Industrial and Engineering Chemistry Research*, vol. 37, no. 10, pp. 3846–3852, 1998.

[29] E. Nurlaela, *Development of Cu-Ni/$TiO_2$ bimetallic catalyst for photohydrogen production under visible light illumination [M.S. thesis]*, Universiti Teknologi PETRONAS, Tronoh, Bandar Seri Iskandar, Malaysia, 2011.

[30] P. Li, J. Liu, N. Nag, and P. A. Crozier, "In situ preparation of Ni-Cu/$TiO_2$ bimetallic catalysts," *Journal of Catalysis*, vol. 262, no. 1, pp. 73–82, 2009.

[31] C.-S. Lu, C.-C. Chen, F.-D. Mai, and H.-K. Li, "Identification of the degradation pathways of alkanolamines with $TiO_2$ photocatalysis," *Journal of Hazardous Materials*, vol. 165, no. 1–3, pp. 306–316, 2009.

[32] X. Zhu, C. Yuan, Y. Bao, J. Yang, and Y. Wu, "Photocatalytic degradation of pesticide pyridaben on $TiO_2$ particles," *Journal of Molecular Catalysis A: Chemical*, vol. 229, no. 1-2, pp. 95–105, 2005.

[33] V. Mirkhani, S. Tangestaninejad, M. Moghadam, M. Habibi, and A. R. Vartooni, "Photodegradation of aromatic amines by Ag-$TiO_2$ photocatalyst," *Journal of the Iranian Chemical Society*, vol. 6, no. 4, pp. 800–807, 2009.

[34] J. C. Yu, J. Lin, D. Lo, and S. K. Lam, "Influence of thermal treatment on the adsorption of oxygen and photocatalytic activity of $TiO_2$," *Langmuir*, vol. 16, no. 18, pp. 7304–7308, 2000.

[35] S. Sakulkhaemaruethai, S. Pavasupree, Y. Suzuki, and S. Yoshikawa, "Photocatalytic activity of titania nanocrystals prepared by surfactant-assisted templating method—effect of calcination conditions," *Materials Letters*, vol. 59, no. 23, pp. 2965–2968, 2005.

[36] L. C. Macedo, D. A. M. Zaia, G. J. Moore, and H. de Santana, "Degradation of leather dye on $TiO_2$: a study of applied experimental parameters on photoelectrocatalysis," *Journal of Photochemistry and Photobiology A: Chemistry*, vol. 185, no. 1, pp. 86–93, 2007.

[37] B. Ma, F. Wen, H. Jiang, J. Yang, P. Ying, and C. Li, "The synergistic effects of two Co-catalysts on $Zn_2GeO_4$ on photocatalytic water splitting," *Catalysis Letters*, vol. 134, no. 1-2, pp. 78–86, 2010.